Mechanical Systems and Signal Processing 161 (2021) 107939

Contents lists available at ScienceDirect

Mechanical Systems and Signal Processing

journal homepage: www.elsevier.com/locate/ymssp

Predicting the seismic collapse capacity of adjacent SMRFs retrofitted with fluid viscous dampers in pounding condition

Farzin Kazemi [a], Benyamin Mohebi [a], Robert Jankowski [b,*]

[a] Department of Civil Engineering, Faculty of Engineering and Technology, Imam Khomeini International University, PO Box 34148-96818, Qazvin, Iran
[b] Faculty of Civil and Environmental Engineering, Gdansk University of Technology, ul. Narutowicza 11/12, 80-233 Gdansk, Poland

ARTICLE INFO

Article history:
Received 24 January 2021
Received in revised form 26 March 2021
Accepted 30 March 2021

Keywords:
Modification factors
Seismic retrofit
Seismic collapse capacity
Fluid viscous dampers
Seismic collapse fragility
Structural pounding
Incremental dynamic analysis

ABSTRACT

Severe damages of adjacent structures due to structural pounding during earthquakes have emphasized the need to use some seismic retrofit strategy to enhance the structural performance. The purpose of this paper is to study the influence of using linear and nonlinear Fluid Viscous Dampers (FVDs) on the seismic collapse capacities of adjacent structures prone to pounding and proposing modification factors to modify the median collapse capacity of structures considering the effects of pounding. The factors can be used to predict the collapse capacity of structures in pounding condition. A seismic retrofit strategy employs FVDs installed in 3-, 6- and 9-story Special Moment Resisting Frames (SMRFs). The SMRFs were assumed to have different values of separation distance according to the seismic code. To model pounding phenomenon, linear viscoelastic contact elements were used in the OpenSees software. Furthermore, to determine the seismic collapse capacities of each structure, the proposed algorithm was applied to remove the collapsed structure during the incremental dynamic analysis. The results of the analyses illustrate that the existence of FVDs can substantially improve the seismic behavior of structures having a significant influence on the collapse capacities of colliding structures. Moreover, considering the adjacent SMRFs in one or two sides of the main structure can significantly affect the median collapse capacity of the main structure itself. Finally, the proposed modification factors can be successfully used to estimate the effects of pounding on the collapse capacities of adjacent structures.

1. Introduction

Different investigations show that adjacent structures with inappropriate separation distance between them may interact one with another during earthquakes, resulting in significant damage [1]. Although nowadays it is a usual procedure to consider a minimum separation distance during the design of concrete or steel structures, many existing structures were constructed with insufficient in-between gap size since it was allowed due to old seismic codes. This insufficient separation distance, which may lead to impacts between adjacent structures during earthquakes, can significantly influence the seismic structural behavior as well as the collapse capacity. Therefore, improving the seismic performance of existing structures is often challenging because such external circumstances can affect the structural behavior. In this respect, there are two strategies: first, increasing the capacity of structural members, for instance using friction devices into beam to column joints,

* Corresponding author.
E-mail address: jankowr@pg.edu.pl (R. Jankowski).

https://doi.org/10.1016/j.ymssp.2021.107939
0888-3270/

and second, installing passive energy dissipation devices such as dampers or adding dissipative metal shear panels (see for instance [2–12]). The first approach is more convenient for low-rise buildings, whereas the second one can be more effective and affordable for all types of structures. Furthermore, the strengthening option for structures may interfere with the architectural plans, while the installation of seismic dampers can play a positive role. Although previous studies were mainly focused on the strengthening option, the idea of using linear and nonlinear Fluid Viscous Dampers (FVDs) for retrofitting structures is not new. Among different passive energy dissipation systems, FVDs have some performance advantages for their ability to reduce both displacements and accelerations, which can be very important for the structures with sensitive components. Moreover, their velocity-dependent behavior makes them capable of dissipating more energy at small deformations [13,14]]. The response of FVDs can be linear or nonlinear, depending on the velocity exponent value, α, which usually varies from 0.15 to 1.0. Bigdeli et al. [15] investigated the optimal arrangement of a limited number of dampers that minimize the inter-story drifts. They showed that increasing the number of dampers would not necessarily improve efficiency. Martinez-Rodrigo and Romero [16] considered the FVDs mounted on the chevron-braced frames with different values of the velocity exponent in order to compare linear and nonlinear FVD devices. They achieved larger reductions in the peak accelerations by using the linear FVDs, whereas increasing the FVDs nonlinearity resulted in smaller damping forces. Moreover, Dall'Asta et al. [17] accomplished a similar trend of results using a probabilistic methodology. Tubaldi et al. [18,19] proposed probabilistic performance-based procedures to quantify the risk reduction, obtained by using viscous and viscoelastic dampers, and to assess the seismic risk associated with pounding between adjacent structures.

Recently, many retrofitting techniques have been introduced to improve the seismic performance of existing structures. Mansoori and Moghadam [20] investigated the possibility of controlling both accelerations and displacements of asymmetric structures. They concluded that the distribution of linear FVDs had a significant effect on structural modal properties. Kim et al. [21] considered a seismic retrofitting scheme to enhance the seismic performance of the special truss moment frame using linear FVDs. They indicated that the seismic performance of the special truss moment frame increased by adding linear FVDs in the case of slight to moderate damage state. Landi et al. [22] proposed a procedure in order to direct the determination of FVDs required for the seismic retrofit of structures without performing several iterations. Furthermore, Landi et al. [23] proposed a simplified probabilistic method for the seismic assessment of nonlinear structures equipped with nonlinear FVDs. Dall'Asta et al. [24] studied the influence of FVD properties on the probabilistic seismic performance and risk assessment. Karavasilis [25] investigated the design capacity assessment of columns in steel moment-resisting frames with linear FVDs. The results of the study indicated that steel moment-resisting frames with linear FVDs were more prone to column plastic hinging, as compared to steel moment-resisting frames. Seismic design and assessment of the steel self-centering moment-resisting frames with FVDs were also investigated by Tzimas et al. [26]. They showed that using FVDs was effective in improving the residual drift performance of steel self-centering moment-resisting frames. Kandemir-Mazanoglu and Mazanoglu [27] as well as Kazemi et al. [28] investigated the effects of using viscous dampers between two adjacent structures. They showed that this approach could be used to substantially improve structural behavior during seismic excitations and to prevent earthquake-induced structural pounding.

Pounding between two adjacent structures is a source of considerable amplification of accelerations in structures. In addition, this phenomenon can substantially modify the structural response [1]. Previous studies reveal that structural characteristics, such as mass and fundamental natural period of the adjacent structure, and the fact of having the single- or double-sided pounding may both increase or decrease the structural response [29–31]. Crozet et al. [32] performed a sensitivity analysis to provide a consistent measure of the relative importance of parameters, such as the coefficient of restitution as well as mass and frequency ratios of the colliding structures, using the Monte Carlo simulations of single-degree-of-freedom (SDOF) systems. It is important to utilize more precise structural models to evaluate pounding phenomenon. Therefore, some researchers used multi-degree-of-freedom (MDOF) models, with the mass of each story concentrated at the floor level [31,33]. Favvata [34] correlated the seismic performance of 3- and 8-story structures with the minimum required separation distance for three intensity levels of seismic hazard. The most important issue in the case of the inter-story pounding conducted in that study was the local performance of exterior columns, which had a critical condition due to impact force. Also, the minimum required separation distance was found to be dependent on the level of the seismic hazard. It is also clear that considering the P-Delta effect can influence the stability of the structure. Moreover, including or excluding the P-Delta effect can result in the increase or decrease in the structural response under ground motions. Therefore, many studies investigated the influence of P-Delta effect on the seismic collapse capacity of structures [35–39]. Masroor and Mosqueda [40] examined the collapse probability of pounding between a base-isolated steel structure and moat wall. They concluded that the collapse margin ratio could be reduced significantly as the result of pounding. Moreover, Elwardany et al. [41,42] studied the effect of the infill panels on the seismic response of adjacent structures prone to collisions. The results showed that the existence of infill panels could significantly affect the pounding-involved structural response during earthquakes.

Nevertheless, despite considerable research in the field of earthquake-induced structural pounding, the results of studies concerning the effectiveness of different methods of modification of collapse capacities of structures, so as to improve their seismic resistance, are very limited. Therefore, the aim of this paper is to study the influence of using linear and nonlinear FVDs on the seismic collapse capacities of adjacent Special Moment Resisting Frames (SMRFs) prone to pounding. Furthermore, to extend the results of the study, comprehensive sensitivity analyses of the earthquake-induced pounding between three adjacent SMRFs are performed to investigate the effect of considering two adjacent structures on collapse capacities of the main structure. Then, the modification factors, intended to estimate the median collapse capacity, are proposed.

Moreover, this paper is focused on the influence of using the linear and nonlinear FVDs on the seismic collapse fragility curves of colliding structures.

2. Description of theoretical aspects

2.1. Nonlinear modeling of structures

3-, and 6-story SMRFs, considered by Kitayama and Constantinou [43], as well as 9-story SMRFs designed according to ASCE/SEI 7-10 [44], were used in the study (see also [28]). Seismic design parameters of SD_S = 1.25 g and SD_1 = 0.6 g were assumed for a site of latitude 37.88°N, longitude 122.08°W, and soil class D. Besides, the response modification factor of R = 8, the deflection amplification factor of C_d = 5.5 and the system over-strength factor of Ω = 3 were selected for SMRFs according to ASCE/SEI 7-10 [44]. The design dead and live loads of roof, taken as equal to 1.68 kN/m^2 and 0.96 kN/m^2, and the floor dead and live loads of 3.35 kN/m^2 and 1.68 kN/m^2 were applied to structures. Also, a cladding load of 1.68 kN/m^2 was considered. Fig. 1 presents a rectangular plane configuration, i.e. a perimeter frame system of the considered building and a concentrated plasticity model for 6-story SMRF. All columns, except for those in the SMRF, were modeled as leaning columns considering the P-Delta effect (see [45–47] for details). At both ends of each beam, a nonlinear rotational spring was considered using zero-length elements, according to the Modified Ibarra–Krawinkler bilinear-hysteretic model [48]. Therefore, based on this approach, each beam in SMRFs was modeled by elastic beam-column element and two zero-length elements located at both ends.

According to Newell and Uang [49], cyclic deterioration does not play a key role in the seismic performance of W14 columns. Therefore, in this study, the nonlinear beam-column element, and *Steel02* material available in OpenSees software, were employed to model all columns. Similar to the studies carried out by Seo et al. [50], as well as by Kitayama and

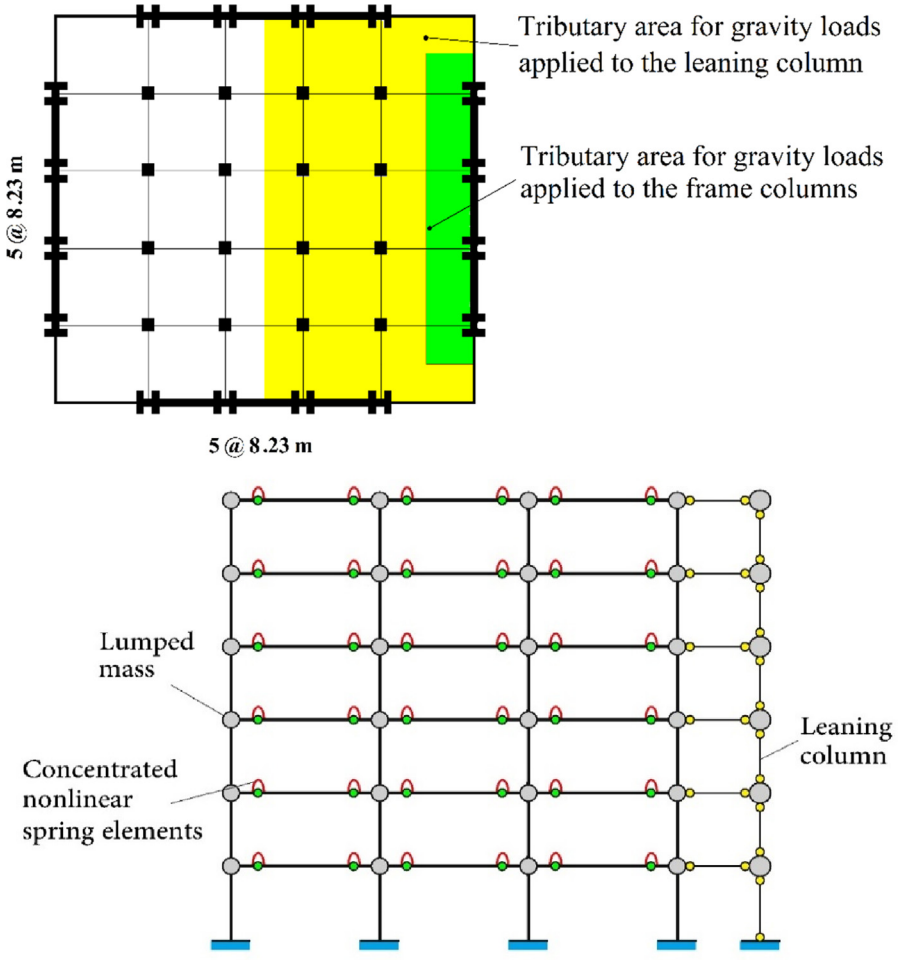

Fig. 1. Structural modeling of the 6-story SMRF, (a) floor plan of building, (b) lumped plasticity model of SMRF.

Constantinou [51], a ratio of elastic to post-elastic stiffness equal to 0.002 was assumed for modeling the uniaxial behavior of columns. Moreover, Fig. 2 depicts the elevation and arrangement of the linear and nonlinear FVDs on 3-, 6-, and 9-story SMRFs, which were placed diagonally.

2.2. Equipping structures with supplemental FVDs

FVDs are velocity-dependent passive energy dissipation devices that can behave as linear or nonlinear elements. The force, F_d, produced by an FVD, depends on the relative velocity between two ends of the damper and is given as follows:

$$F_d = C(\alpha) \cdot |v|^{\alpha} \cdot \mathrm{sgn}(v) \tag{1}$$

where $C(\alpha)$ is the damping coefficient, v is the relative velocity between two ends of the FVD, α is the velocity exponent, and sgn is the signum function. The device behaves as a linear FVD for $\alpha = 1$, and behaves as a nonlinear FVD for the values of lower than one. Landi et al. [22,52] introduced a method based on the comparison between the demand spectrum and capacity spectrum. The capability of the structure to dissipate the seismic input energy is presented with the effective damping of a structure equipped with the FVDs and can be determined as follows:

$$\xi_{eff} = \xi_h + \xi_D + \xi_i \tag{2}$$

where ξ_h represents the hysteretic damping ratio of the structural elements, ξ_D is the supplemental damping ratio provided by the FVDs with nonlinear structural behavior and ξ_i is the inherent damping ratio. To compute the effective damping, ξ_{eff}, the demand spectrum should be compared with the capacity spectrum of the structure, as derived from the base shear-roof displacement curve using nonlinear static pushover analysis. Therefore, for the transformation of the base shear-roof displacement curve into the capacity spectrum, the relations proposed by Landi et al. [22,52] were used. The supplemental viscous damping ratio for the first mode of vibration, ξ_D, can be calculated as follows:

$$\xi_D = \frac{\sum_{i=1}^{Nd} (2\pi)^{\alpha} \cdot T_1^{2-\alpha} \cdot \lambda_i \cdot C_i \cdot f_i^{1+\alpha} \cdot D_{roof}^{\alpha-1} \cdot \varphi_{ri1}^{1+\alpha}}{8\pi^3 \cdot \sum_{j=1}^{Ns} m_j \cdot \varphi_{j1}^2} \tag{3}$$

where N_d is the number of the FVD devices, T_1 is the fundamental period of the first mode of vibration, λ_i is a constant value depending on the exponent of velocity α, C_i is the damping coefficient of ith FVD, $f_i = \cos\theta_i$ is the amplification factor related to the geometrical arrangement of the FVDs, θ_i is the angle of FVD direction with the horizontal axis, D_{roof} is the amplitude of the roof displacement, φ_{ri1} is the relative deformation between the horizontal degrees of freedom at the ends of the ith damper corresponding to the first mode shape, N_s is the number of stories, and m_j and φ_{j1} are the mass of the jth story and the first mode component at the top of the jth story. It is clear that a suitable FVDs distribution can lead to better seismic performance of structures. In this study, a uniform vertical distribution of damping coefficients were selected to enhance the seismic performance of structures [52,53]. The values of ξ equal to 0.109, 0.094 and 0.128, obtained from Eq. (3), were considered for the 3-, 6-, and 9-story SMRFs, respectively, assuming a maximum inter-story drift ratio of 0.015, as for the design

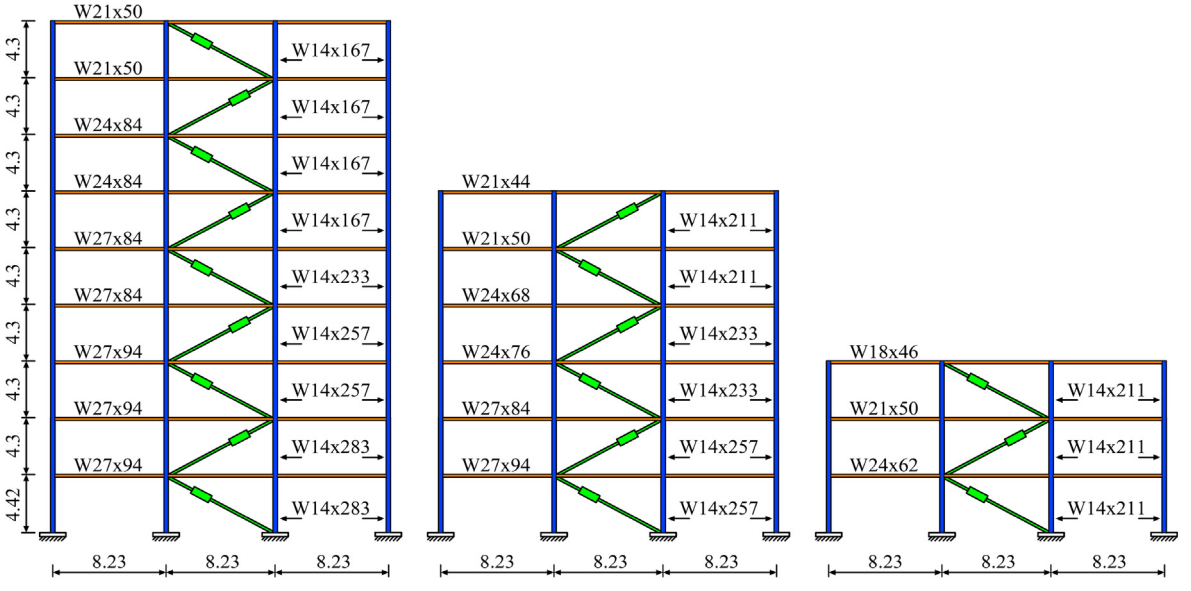

Fig. 2. Elevation and arrangement of the linear and nonlinear FVDs on the 3-, 6-, and 9-story SMRFs.

Table 1
Models considered in the analysis and the separation distance (SD) between adjacent structures.

Structures considered in model	SD = 0.0 (m)	SD = 0.5D (m)	SD = 1.0D (m)
3-story reference	–	–	–
6-story reference	–	–	–
9-story reference	–	–	–
3-story reference and 6-story reference	0.0	0.149	0.298
3-story reference and 9-story reference	0.0	0.173	0.345
6-story reference and 9-story reference	0.0	0.216	0.431
3-story-FVD and 6-story reference	0.0	0.149	0.298
3-story-FVD and 9-story reference	0.0	0.173	0.345
6-story-FVD and 3-story reference	0.0	0.149	0.298
6-story-FVD and 9-story reference	0.0	0.216	0.431
9-story-FVD and 3-story reference	0.0	0.173	0.345
9-story-FVD and 6-story reference	0.0	0.216	0.431
3-story-FVD and 6-story-FVD	0.0	0.149	0.298
3-story-FVD and 9-story-FVD	0.0	0.173	0.345
6-story-FVD and 9-story-FVD	0.0	0.216	0.431

earthquake according to ASCE/SEI 7-10 [44]. Moreover, it was assumed that the supporting brace member is rigid during seismic loads and the FVDs do not reach their stroke limits [54].

2.3. Procedure for modeling pounding phenomenon

During decades, experimental and numerical studies on earthquake-induced structural pounding have been performed using different structural models and various models of collisions [55–57]. It has been shown that a nonlinear gap element, composed of spring in parallel with a viscous damper, can be successfully used to simulate pounding with acceptable accuracy [58]. According to these studies, the linear viscoelastic model (Kelvin-Voigt model), which is only active in compression, was developed and implemented in the OpenSees software [59] to model the structural pounding phenomenon. The general formula for the pounding force during structural impact is expressed as:

$$F(t) = K_k\delta(t) + C_k\dot{\delta}(t) \tag{4}$$

where K_k, $\delta(t)$, C_k and $\dot{\delta}(t)$ denote the impact stiffness coefficient between colliding structures, the relative deformation of pounding element, the impact damping coefficient, and the relative velocity of pounding element, respectively. The damping coefficient of impact element, which accounts for the energy dissipation during pounding, can be obtained as follows [50,60,61]:

$$C_k = 2\xi\sqrt{K_k\frac{m_i m_j}{m_i + m_j}} \tag{5}$$

$$\xi = \frac{-ln\ (e)}{\sqrt{\pi^2 + (ln\ (e))^2}} \tag{6}$$

where m_i, m_j are masses of structures and ξ is the impact damping ratio correlated with a well-known coefficient of restitution, e [58]. The coefficient of restitution is equal to the ratio between the post-impact and the prior-impact relative

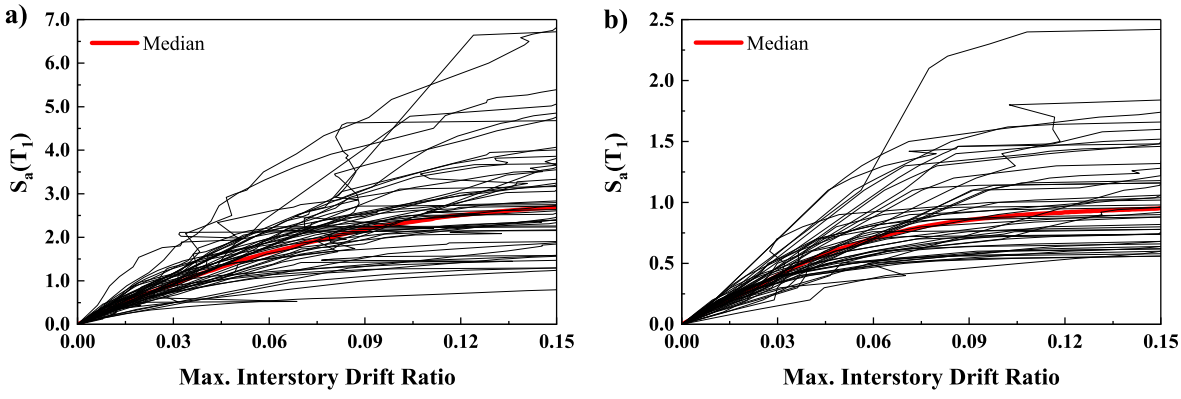

Fig. 3. IDA curves of the 3-, and 6-story reference colliding structures with separation distance of 0.0.

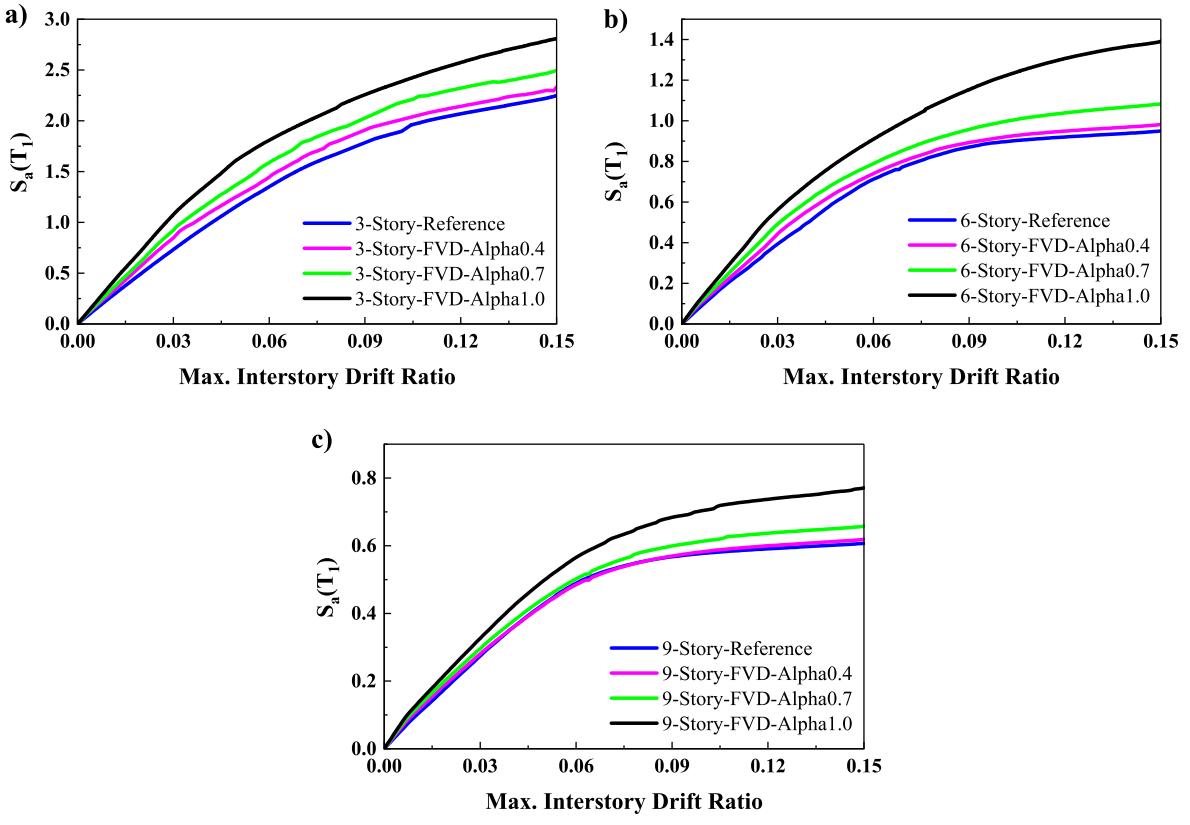

Fig. 4. Median collapse capacities of the 3-, 6-, and 9-story reference structures without any adjacent structure equipped linear or nonlinear FVDs.

velocities of colliding structures. According to previous studies, for concrete-to-concrete impact, the coefficient of restitution is usually taken to be equal to 0.65 [58,62].

Simple modeling and accounting for the energy dissipation during pounding make the linear viscoelastic contact element attractive to simulate the pounding phenomenon. Therefore, several studies were performed to calculate the impact stiffness of pounding models which can be affected by the material properties. For example, Polycarpou et al. [63] considered a simple approximation to determine the stiffness value of impact element, which depends on the material characteristics and the plan geometry in the vicinity of impact. Thus, using the area of the overlapping region in the impacted vicinity, the normal impact stiffness, K_{imp}, can be approximated as follows:

$$K_{imp} = \left[\frac{1-\nu_1^2}{E_{Dynamic,1}} + \frac{1-\nu_1^2}{E_{Dynamic,2}}\right]^{-1} \tag{7}$$

$$E_{Dynamic,\ i} = 5.82\left(E_{Static,\ i}\right)^{0.63}, \quad \text{in GPa} \tag{8}$$

where ν_i is the Poisson's ratio for the i-th structure, and $E_{Dynamic,i}$ is the dynamic modulus of elasticity of normal strength concrete that is calculated based on the static modulus of elasticity, $E_{Static,i}$, according to the results of an experimental work performed by Salman and Al-Amawee [64]. Assuming E_{Static} = 21 GPa and ν = 0.2, based on [63,65], the normal impact stiffness was calculated from Equation (7) to be equal to $K_{imp} = 20.96 \times 10^6$ kN/m^2. Therefore, the impact stiffness, K_k, was determined to be 4.31×10^{11} kN/m by multiplying the normal impact stiffness, $K_{imp,}$ by half of the length of the pounding side of

Table 2
Median collapse capacities of the 3-, 6-, and 9-story reference structures without any adjacent structure.

Structure	Reference	$\alpha = 0.4$	$\alpha = 0.7$	$\alpha = 1.0$
3-story	2.25	2.33	2.50	2.81
6-story	0.95	0.98	1.08	1.39
9-story	0.61	0.62	0.66	0.77

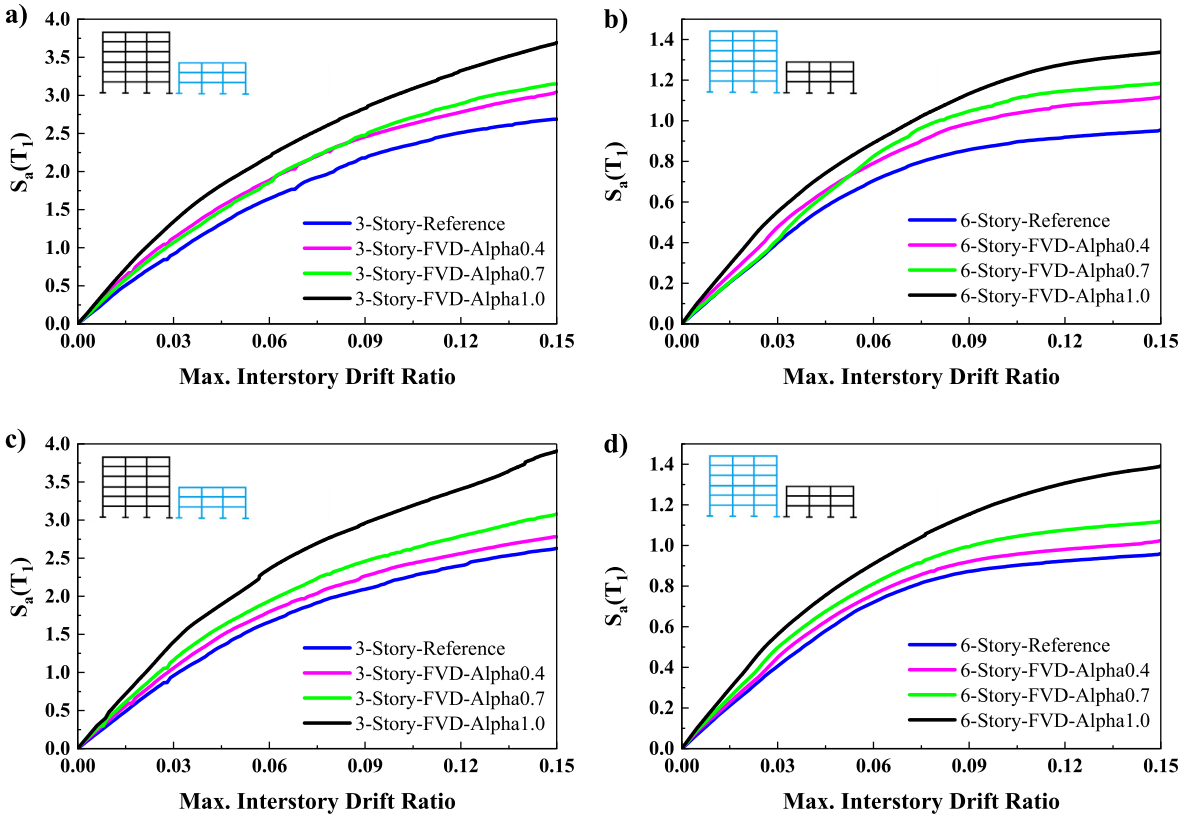

Fig. 5. Median collapse capacities of the 3-, and 6-story colliding structures with and without considering FVDs, (a) and (b) for the separation distance equal to 0.0, (c) and (d) for the separation distance equal to 1.0D.

the plan, L/2 = 20.575 m. Also, the impact damping coefficient of C_k = 6798.84 kNs/m was obtained from Equation (5), considering the coefficient of restitution equal to e = 0.65.

2.4. Structural models

In crowded cities, where the land space is expensive and limited, the seismic pounding between adjacent buildings is an important issue. So, to minimize the seismic pounding risk, seismic codes provide analytical rules and numerical procedures to estimate the minimum separation distance required for adjacent structures to prevent seismic pounding between them. According to ASCE/SEI 7-10 [44], the minimum separation distance, δ_{MT}, is given as follows:

$$\delta_{MT} = \sqrt{\left(\frac{C_d.\delta_{max}}{I}\right)_1^2 + \left(\frac{C_d.\delta_{max}}{I}\right)_2^2} \tag{9}$$

where δ_{MT} is the maximum inelastic displacement, C_d is the deflection amplification factor (as in Table 12-2-1 of ASCE/SEI 7-10), δ_{max} is the maximum elastic displacement (section 12.8.4.3 of ASCE/SEI 7-10), I is the importance factor. Therefore, the required separation distance, D, should be at least equal to δ_{MT}.

Table 1 presents all the cases studied and the separation distance between them. To evaluate the seismic collapse capacities of colliding structures, three values of separation distance, equal to 0.0, 0.5D, and 1.0D, and three values of velocity exponent, α, equal to 0.4, 0.7, and 1.0, were assumed. In other words, 9 models without supplemental FVDs and 27 models with supplemental FVDs were considered for the analysis of pounding between two structures.

3. Results of analysis

3.1. Evaluating results of using FVDs in BOTH colliding structures

In the study, the Incremental Dynamic Analysis (IDA) was carried out to assess the seismic collapse capacities of colliding structures using MATLAB [66] and OpenSees [59] software, considering the Hunt and Fill algorithm to capture the seismic

collapse of structures [67]. IDA is a technique to assess the seismic collapse capacities of structures utilizing a series of nonlinear dynamic analyses. Using appropriate intensity parameters is an important aspect of a study which was considered by Kita et al. [68] who applied Intensity Measures (IMs) computed from seismic data. Recently, three advanced scalar IMs, which include information about the spectral shape and ground motion duration, have been proposed by Jamshidiha et al. [54]. These IMs had better performance in predicting the collapse capacity of SMRFs equipped with FVDs, as compared to other well-known IMs. In this study, the scalar intensity measure, $S_a(T_1)$, selected as IM, was increased until the occurrence of the total seismic collapse and the maximum inter-story drift ratio used to measure the structural response. A set of 48 near-field ground motion records were used to perform IDAs (see also [69]). The seismic structural collapse was displayed by the flat part of each IDA curves. In the real world, it does not resist deformations of the adjacent structures when one of them reaches its collapse capacity. Therefore, in the numerical modeling, the collapsed structure should be removed to consider this effect. Due to the seismic collapse of one structure in the pounding models, it is difficult to assess seismic collapse capacities of both colliding structures in the analysis. Thus, an algorithm was developed for the automated removal of the first collapsed structure during the analysis to assess the seismic collapse capacities of both colliding structures. Then, the analysis continued until the seismic collapse of the second structure. This algorithm reduced the time of analysis and considered the effects of collapsed structure in pounding phenomenon. Fig. 3(a)–(b) presents the IDA curves of the 3-, and 6-story reference colliding structures, respectively, with separation distance equal to 0.0.

Fig. 4 presents the median collapse capacities of the 3-, 6-, and 9-story reference structures without any adjacent structure equipped with linear or nonlinear FVDs. It can be seen that the median collapse capacity shows an increasing trend using linear or nonlinear FVDs.

In other words, adding FVDs with values of velocity exponent equal to 0.4, 0.7 and 1.0 to the 3-story reference structure leads to the increase in the median collapse capacity by 4%, 11%, and 24%, respectively. Furthermore, in this case, the median collapse capacity of the 6-story reference structure increases by 3%, 14%, and 46%, and the median collapse capacity of the 9-story reference structure increases by 2%, 8%, and 26%, respectively. Table 2 compares the median collapse capacities of the 3-, 6-, and 9-story reference structures without any adjacent one.

Fig. 5(a)–(b) presents the median collapse capacities of the 3-, and 6-story colliding structures equipped with linear and nonlinear FVDs for the separation distance of 0.0, and Fig. 5(c)–(d) present s these structures for the separation distance

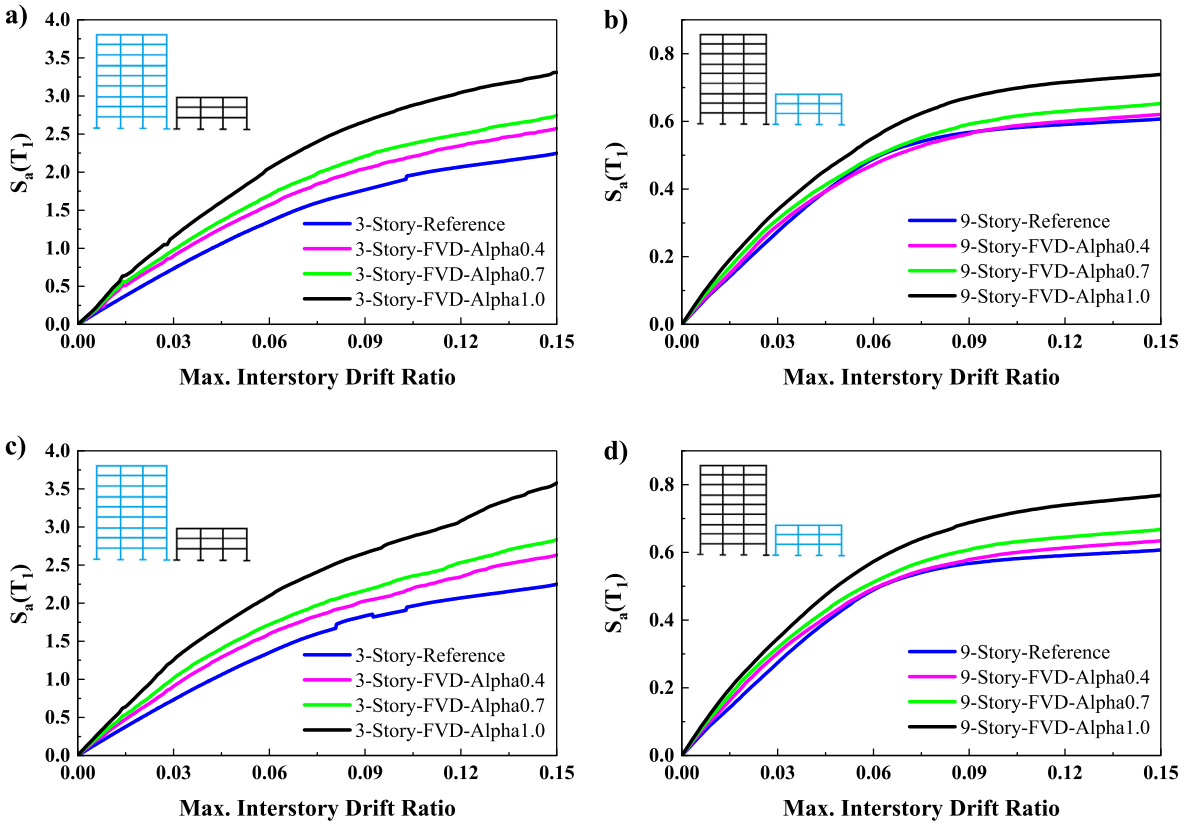

Fig. 6. Median collapse capacities of the 3-, and 9-story colliding structures with and without considering FVDs, (a) and (b) for the separation distance equal to 0.0, (c) and (d) for the separation distance equal to 1.0D.

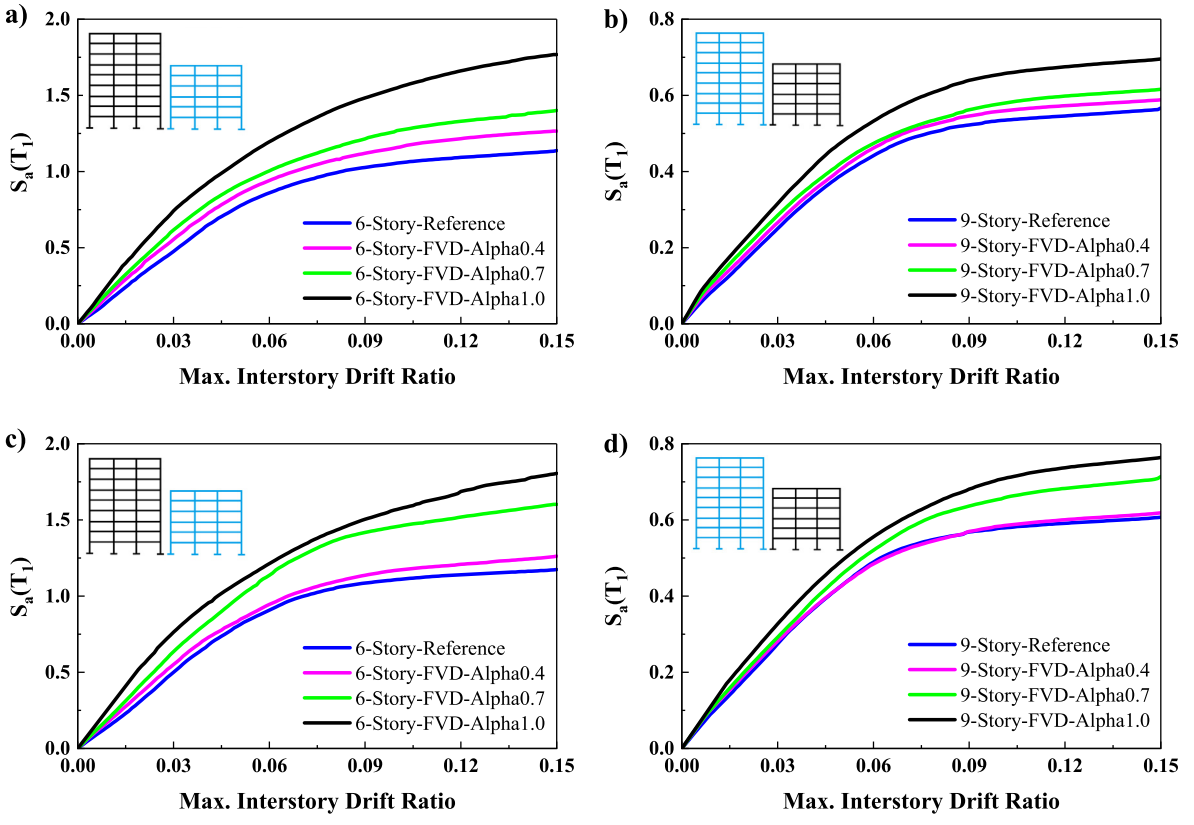

Fig. 7. Median collapse capacities of the 6-, and 9-story colliding structures with and without considering FVDs, (a) and (b) for the separation distance equal to 0.0, (c) and (d) for the separation distance equal to 1.0D.

Table 3
Median collapse capacities of the 3-, 6-, and 9-story colliding structures with two separation distances equal to 0.0 and 1.0D.

Structure	Damper velocity exponent (α)	Pounding with			
		SD=0.0	SD=1.0D	SD=0.0	SD=1.0D
		6-story reference		9-story reference	
3-story reference	-	2.687 →	2.629	2.249 →	2.239
3-story-FVD	0.4	3.045	2.779	2.573	2.634
	0.7	3.151	3.080	2.747	2.837
	1.0	3.693	3.908	3.309	3.579
		3-story reference		9-story reference	
6-story reference	-	0.954 →	0.960	1.157 →	1.134
6-story-FVD	0.4	1.116	1.023	1.275	1.261
	0.7	1.185	1.119	1.401	1.602
	1.0	1.339	1.392	1.767	1.805
		3-story reference		6-story reference	
9-story reference	-	0.607 →	0.617	0.566 →	0.607
9-story-FVD	0.4	0.620	0.634	0.588	0.618
	0.7	0.652	0.668	0.615	0.713
	1.0	0.738	0.769	0.695	0.764

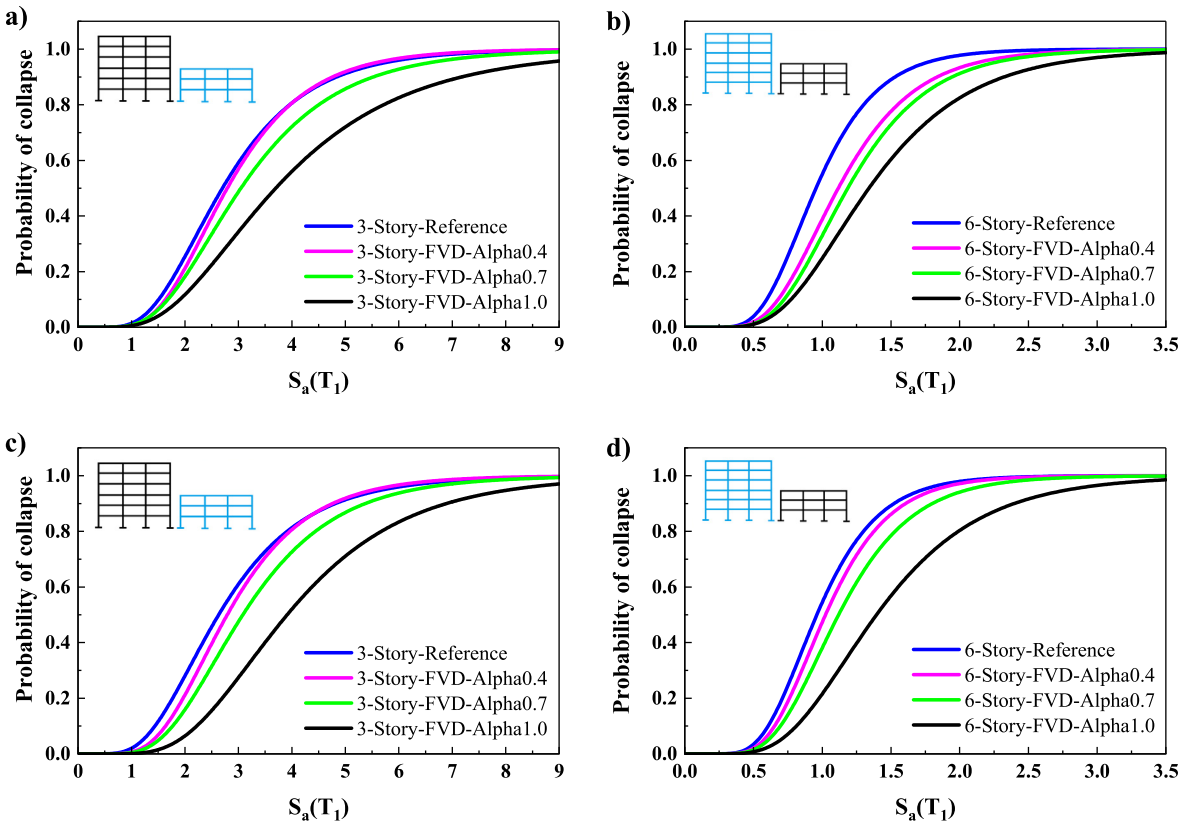

Fig. 8. Seismic collapse fragility curves for the 3-, and 6-story colliding structures, (a) and (b) for the separation distance equal to 0.0, (c) and (d) for the separation distance equal to 1.0D.

equal to 1.0*D*. It can be seen that for the increase in the values of velocity exponent from 0.4 to 1.0, the median collapse capacity of the 3-, and 6-story colliding structures also increases. A similar conclusion can also be drawn from Figs. 6(a)–(d) and 7(a)–(d), which show the median collapse capacities of the 3-, and 9-story colliding structures and the 6-, and 9-story colliding structures, respectively.

Table 3 illustrates the values of the median collapse capacities of the aforementioned colliding structures. The blue and red arrows show an increasing and decreasing trend, respectively. According to the results, adding FVDs leads to the increase in the median collapse capacities of all colliding structures. For example, in the case of pounding between the 3-, and 6-story-FVD structures with $\alpha = 1.0$, for the separation distance of 0.0, the median collapse capacity of the 3-story-FVD structure is 1.21 and 1.17 times larger than the values obtained from the case assuming $\alpha = 0.4$ and 0.7, respectively, while the median collapse capacity of the 6-story-FVD structure is 1.20 and 1.13 times larger than the values obtained from the case assuming $\alpha = 0.4$ and 0.7, respectively. Besides, for the separation distance equal to 1.0*D*, the median collapse capacity of the 3-story-FVD structures is 1.40 and 1.26 times larger than the values obtained from the case assuming $\alpha = 0.4$ and 0.7, respectively, whereas the median collapse capacity of the 6-story-FVD structures is 1.36 and 1.24 times larger than the values obtained from the case assuming $\alpha = 0.4$ and 0.7, respectively. Furthermore, the results indicate that the median collapse capacity of the shorter structure decreases in the case of pounding between a short structure and a taller one (i.e. the 3-story and 9-story colliding structures), as the separation distance between structures rises from 0.0 to 1.0D; while, the median collapse capacity of the taller one increases correspondingly. This result can be observed by following the color and direction of arrows.

Fig. 8(a)–(b) present the seismic collapse fragility curves of the 3-, and 6-story colliding structures equipped with FVDs for the separation distance of 0.0, and Fig. 8(c)–(d) show the seismic collapse fragility curves of the 3-, and 6-story colliding structures for the separation distance equal to 1.0*D*. In comparison between colliding structures with and without FVDs, the seismic collapse probabilities of structures with FVDs are lower than those for structures without FVDs. It is worth mentioning that the colliding structures with nonlinear FVDs have higher seismic collapse probabilities than those of the colliding structures with linear FVDs. Therefore, in the case of colliding structures, linear FVDs have better seismic performance. The same conclusion can be drawn from Figs. 9(a)–(d) and 10(a)–(d), which present the seismic collapse fragility curves of the 3-, and 9-story colliding structures and the 6-, and 9-story colliding structures equipped with FVDs, respectively.

3.2. Evaluating results of using FVDs in one colliding structure

Fig. 11 presents the median collapse capacities of the 3-, and 6-story colliding structures for the case when the taller structure is equipped with linear FVDs and a separation distance is equal to 0.0. The results show that using linear FVDs in the taller structure increases the median collapse capacities of both structures.

A similar pattern is seen in Figs. 12 and 13, which illustrate the 3-, and 9-story colliding structures and the 6-, and 9-story colliding structures equipped with linear FVDs for the separation distance of 0.0, respectively. In other words, in the case of pounding between 3-, and 6-story structures, the median collapse capacities are 1.13 and 1.47 times larger than those without considering linear FVDs, respectively; while in the case of pounding between 3-, and 9-story structures, the median collapse capacities are 1.07 and 1.18 times larger than those without considering linear FVDs, respectively. Also, in the case for 6-, and 9-story colliding structures, the median collapse capacities are 1.08 and 1.17 times larger than those without considering linear FVDs, respectively.

Fig. 14 presents the median collapse capacities of the 3-, and 6-story colliding structures for the case when the shorter structure is equipped with linear FVDs given the separation distance of 0.0. It can be seen that adding linear FVDs to the 3-story structure increases the median collapse capacity of the shorter structure. However, the median collapse capacity of the 6-story structure remains unchanged. Moreover, a similar pattern can be seen in Fig. 15 for the case of pounding between the 3-, and 9-story structures.

Table 4 summarizes the results derived from Figs. 11–15 showing the median collapse capacities of the 3, 6-, and 9-story colliding structures for the case when one structure is equipped with linear FVDs given the separation distance of 0.0.

3.3. Evaluating results of pounding between three structures

This section evaluates the effects of considering pounding between one structure (the main one) and two adjacent structures at one or two sides. The seismic collapse capacities of the main structure were compared with the case of the single structure without any interactions with other structures. An automated algorithm was used to assess the seismic collapse capacities of each of the structures by removing the collapsed structure during the analysis. Therefore, in each model including pounding between three adjacent structures, the algorithm was used to obtain three IDA curves corresponding to the specific ground motion record. Fig. 16 presents the median collapse capacity and the seismic collapse fragility curve of

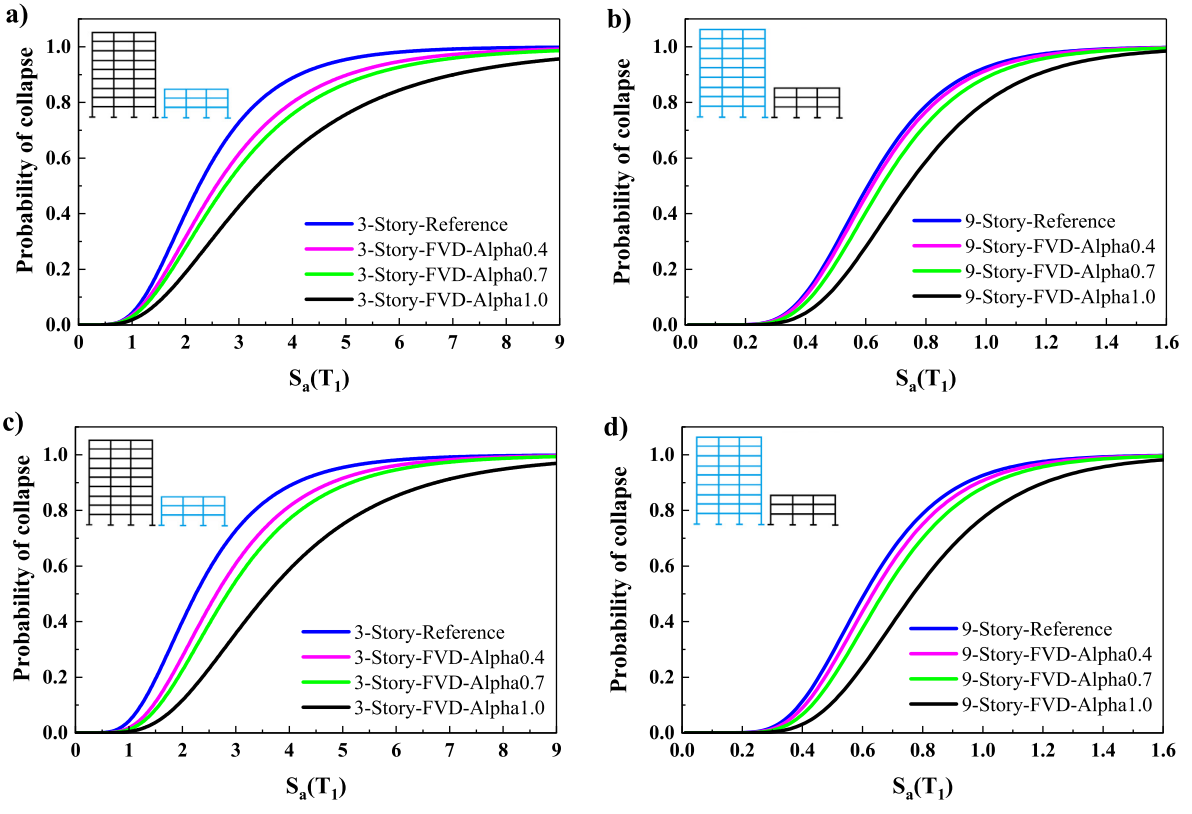

Fig. 9. Seismic collapse fragility curves for the 3-, and 9-story colliding structures, (a) and (b) for the separation distance equal to 0.0, (c) and (d) for the separation distance equal to 1.0D.

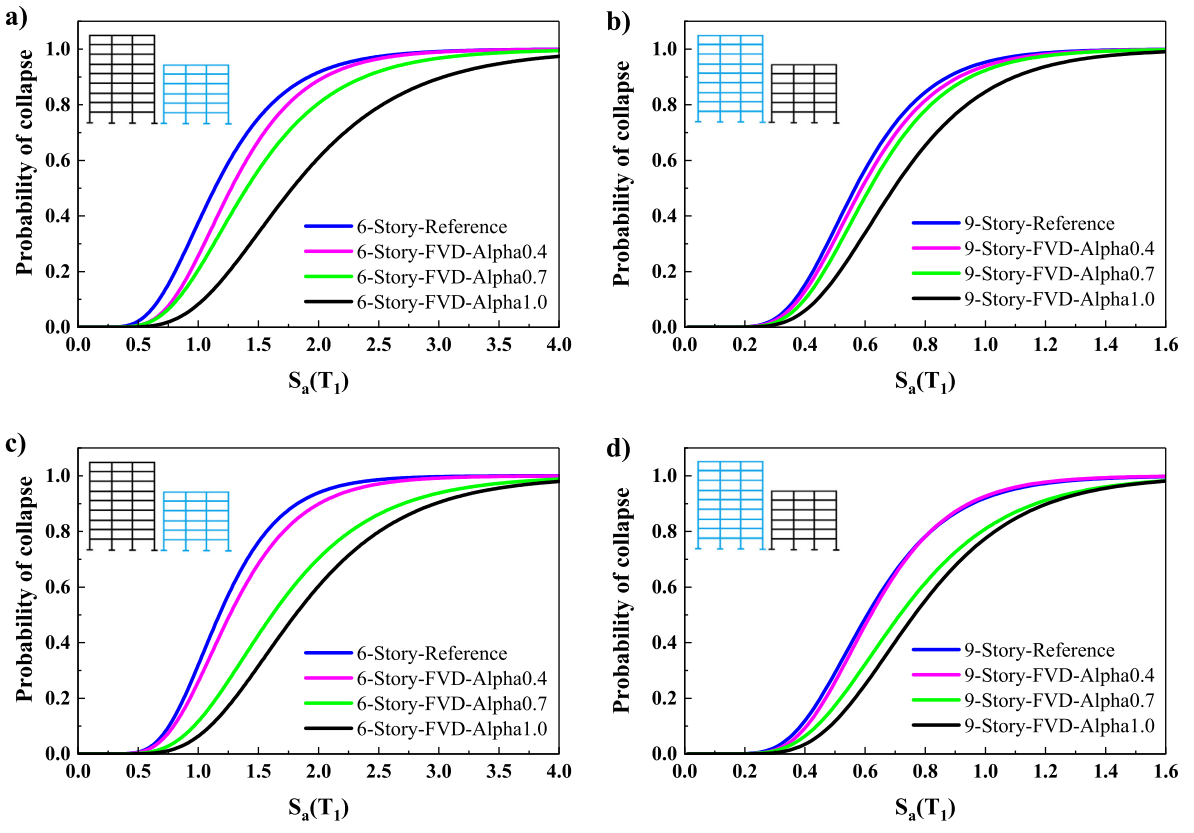

Fig. 10. Seismic collapse fragility curves for the 6-, and 9-story colliding structures, (a) and (b) for the separation distance equal to 0.0, (c) and (d) for the separation distance equal to 1.0D.

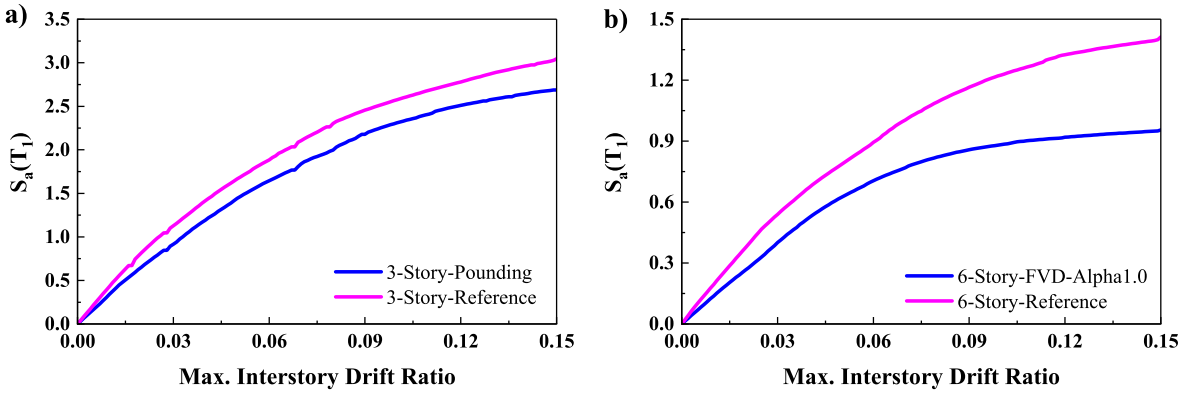

Fig. 11. Median collapse capacities of the 3-, and 6-story colliding structures considering linear FVDs for taller structure given the separation distance of 0.0.

the main 6-story reference structure colliding with two adjacent 3-story structures given the separation distance of 1.0*D*. Comparing to the single 6-story reference structure, considering two adjacent 3-story structures at both sides of the main 6-story reference structure increases (up to 8%) the median collapse capacity of the main structure. Moreover, the seismic collapse probability of the main 6-story reference structure was considerably smaller in comparison with the main 6-story reference structure without any adjacent structure. So, considering two adjacent structures at both sides can increase the median collapse capacity of the main structure, and can decrease the probability of its collapse.

According to the results shown in Figs. 17–19, which present different combinations between three adjacent structures, considering two adjacent structures on both sides of the main structure can improve the seismic performance of the main structure, apart from the fact that the main structure is shorter or taller than the adjacent structures. For example, the med-

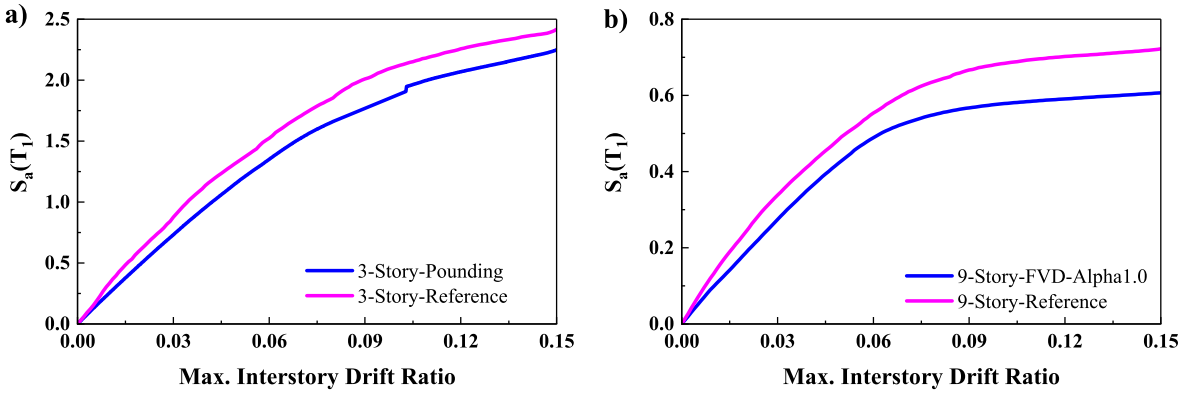

Fig. 12. Median collapse capacities of the 3-, and 9-story colliding structures considering linear FVDs for taller structure given the separation distance of 0.0.

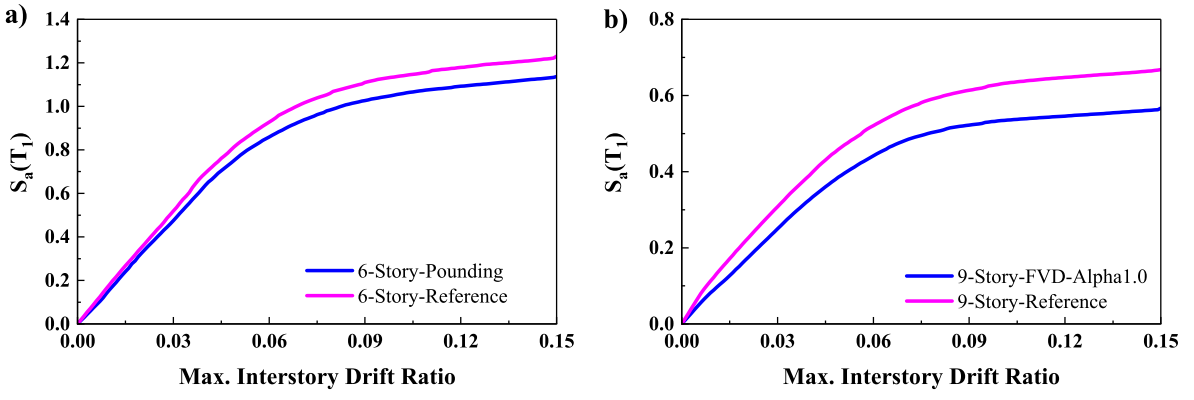

Fig. 13. Median collapse capacities of the 6-, and 9-story colliding structures considering linear FVDs for taller structure given the separation distance of 0.0.

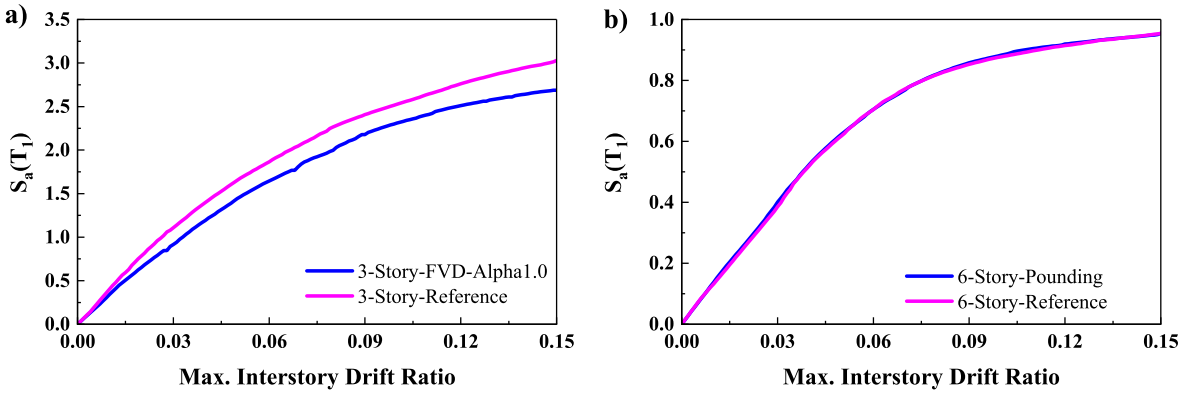

Fig. 14. Median collapse capacities of the 3-, and 6-story colliding structures considering linear FVDs for shorter structure given the separation distance of 0.0.

ian collapse capacity of the main 9-story reference structure colliding with two adjacent 3-story structures at both sides is 1.08 times larger than the value for the single main 9-story-reference structure. Also, the median collapse capacity of the main 3-story reference structure colliding with two adjacent 9-story structures at both sides is 1.17 times larger than the value for the single main 3-story reference structure.

Fig. 20 presents the median collapse capacity and the seismic collapse fragility curve of the main 9-story reference structure colliding with two adjacent 3-story structures at one side of the main structure. It can be seen that considering two adjacent structures at one side of the main structure significantly decreases the median collapse capacity of the 9-story reference

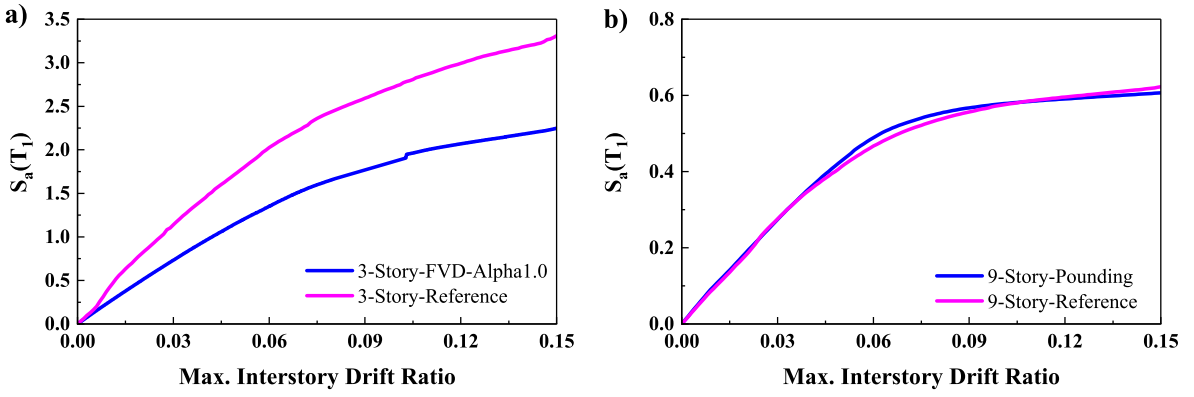

Fig. 15. Median collapse capacities of the 3-, and 9-story colliding structures considering linear FVDs for shorter structure given the separation distance of 0.0.

Table 4
Median collapse capacities of the 3, 6-, and 9-story colliding structures for the case when one structure is equipped with linear FVDs given the separation distance of 0.0.

Structure	3-story-Reference	6-story-Reference	9-story-Reference	3-story-FVD	6-story-FVD	9-story-FVD
3-story-Reference	–	2.687	2.249	–	2.702	2.417
6-story-Reference	0.954	–	1.157	0.964	–	1.230
9-story-Reference	0.607	0.566	–	0.622	0.589	–
3-story-FVD	–	3.737	3.309	–	3.693	3.309
6-story-FVD	1.412	–	1.713	1.339	–	1.767
9-story-FVD	0.722	0.668	–	0.738	0.695	–

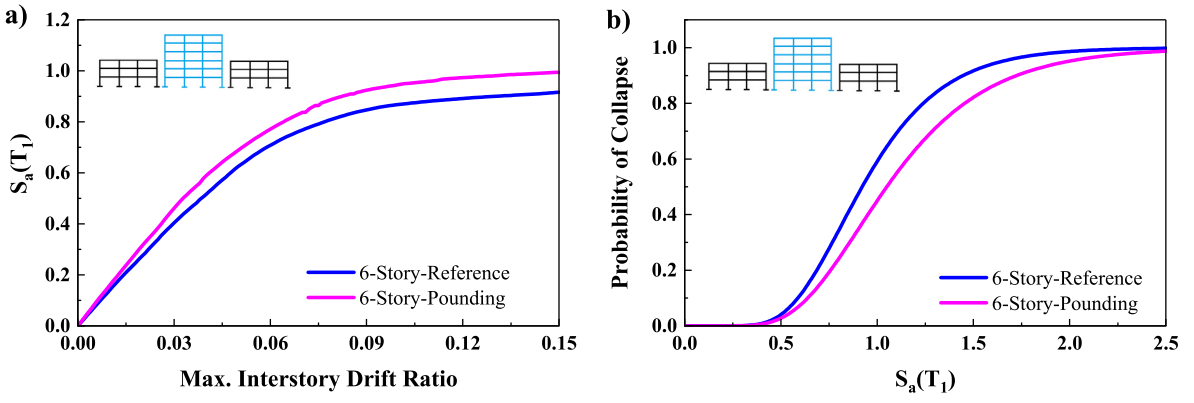

Fig. 16. Comparing median collapse capacity and seismic collapse fragility curve for the 6-story reference structure colliding with two adjacent 3-story structures for the separation distance of 1.0D.

structure. In addition, in this situation, the 9-story reference colliding structure has a higher seismic probability of collapse than the single 9-story reference structure. Thus, it can be concluded that the existence of two structures at one side of the main structure can decrease the seismic performance of the main structure itself.

Table 5 summarizes the results derived from Figs. 16–20 showing the median collapse capacity and seismic collapse fragility (50% probability) for the main structure having different adjacent structures at both sides given the separation distance of 0.0 and 1.0D.

4. Modification factors

In this section, the modification factors of all colliding structures are presented. It should be underlined that the modification factors can be used to modify the collapse capacity of structures due to pounding. In other words, having the amount of collapse capacity of the structure without pounding, the effect of pounding can be considered to assess the collapse capac-

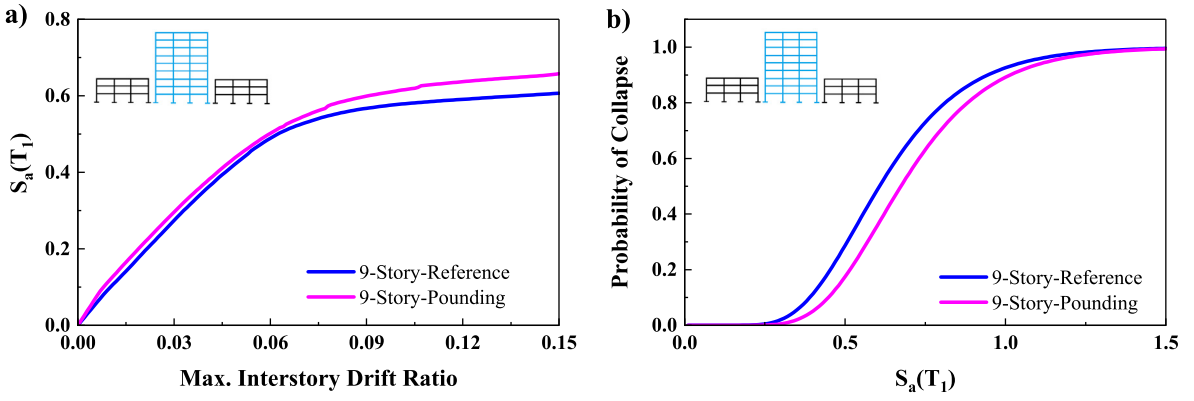

Fig. 17. Comparing median collapse capacity and seismic collapse fragility curve for the 9-story reference structure pounding with two adjacent 3-story reference structures for the separation distance of 0.0.

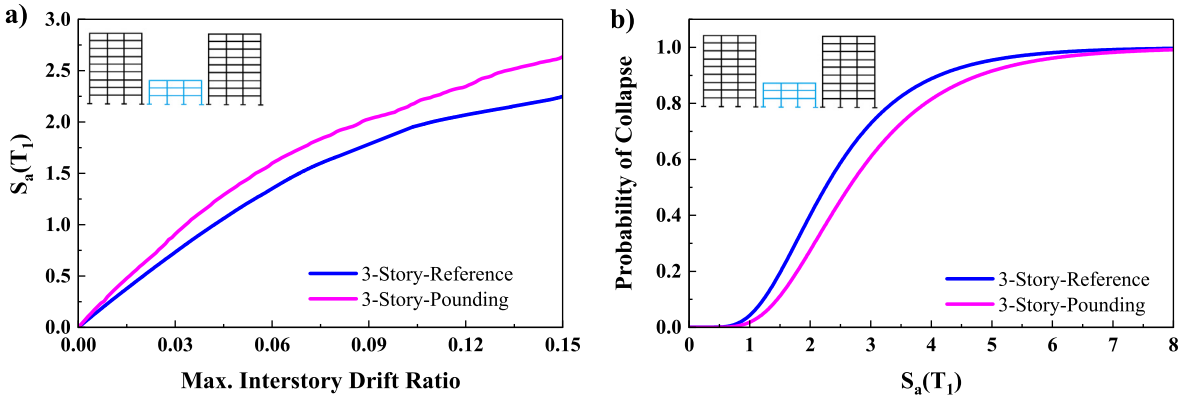

Fig. 18. Comparing median collapse capacity and seismic collapse fragility curve for the 3-story reference structure colliding with two adjacent 9-story structures for the separation distance of 0.0.

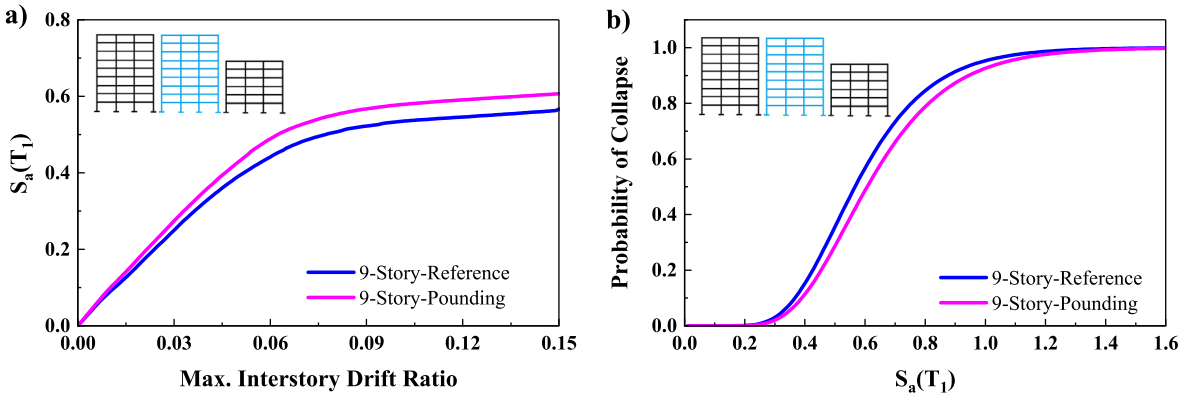

Fig. 19. Comparing median collapse capacity and seismic collapse fragility curve for the 9-story reference structure colliding with two adjacent 6-, and 9-story structures for the separation distance of 0.0.

ity of adjacent structures. This can considerably reduce the efforts to capture collapse capacities. Therefore, the modification factors are proposed to be used as an initial guide to estimate the influence of pounding on the collapse capacity of adjacent structures. By using the modification factors, we can approximately predict the collapse capacity of the structure due to changing its conditions, such as constructing new structures in the vicinity of an existing one or retrofitting structures with linear or nonlinear FVDs. In the case of collisions with the existing adjacent structure having the modification factor greater than one, no modification factor must be applied because neglecting the pounding effects is a conservative assumption.

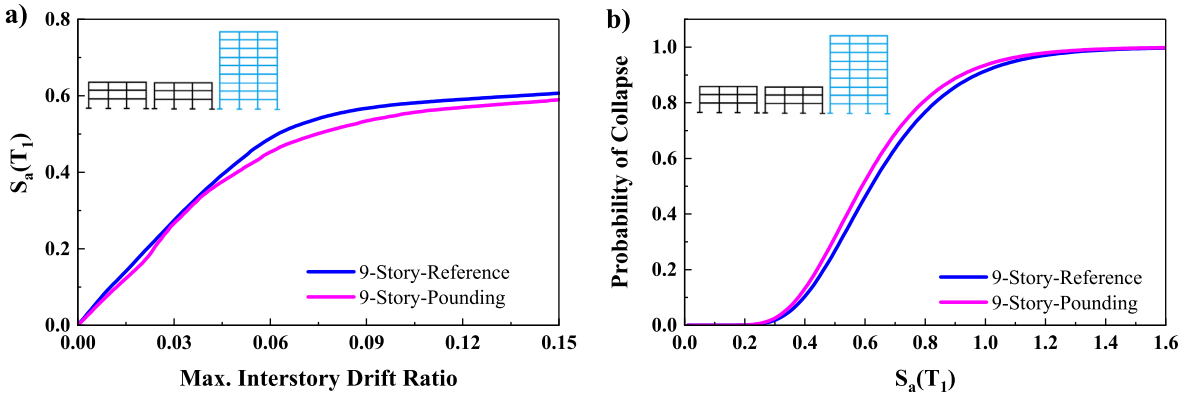

Fig. 20. Comparing median collapse capacity and seismic collapse fragility curve for the 9-story reference structure colliding with two adjacent 3-story structures for the separation distance of 0.0.

Table 5
Median collapse capacity and seismic collapse fragility (50% probability) for the main structure having different adjacent structures at both sides given the separation distance of 0.0 and 1.0D.

Main Structure	Median collapse capacity			Seismic collapse fragility (50%)		
	Left Structure	Middle Structure	Right Structure	Left Structure	Middle Structure	Right Structure
6-story-Reference	3-story-Reference	0.994	3-story-Reference	3-story-Reference	0.994	3-story-Reference
9-story-Reference	3-story-Reference	0.657	3-story-Reference	3-story-Reference	0.657	3-story-Reference
3-story-Reference	9-story-Reference	2.651	9-story-Reference	9-story-Reference	2.651	9-story-Reference
9-story-Reference	9-story-Reference	0.639	6-story-Reference	9-story-Reference	0.639	6-story-Reference
9-story-Reference	3-story-Reference	3-story-Reference	0.589	3-story-Reference	3-story-Reference	0.589

Table 6
Modification factors of the 3-, 6- and 9-story reference structures colliding with an adjacent structure for the separation distances equal to 0.0 and 1.0D.

Structure	α	Adjacent structure							
		SD		SD		SD		SD	
		0.0	1.0D	0.0	1.0D	0.0	1.0D	0.0	1.0D
		6-story-FVD		6-story reference		9-story-FVD		9-story reference	
3-story reference	-	1.353	1.312	1.194	1.168	1.074	1.083	0.999	0.995
3-story-FVD	0.4	1.306	1.192	1.180	1.123	1.104	1.130	1.060	1.031
	0.7	1.260	1.232	1.212	1.119	1.098	1.134	1.092	1.074
	1.0	1.314	1.390	1.078	1.067	1.177	1.273	1.177	1.163
		3-story-FVD		3-story reference		9-story-FVD		9-story reference	
6-story reference	-	1.014	1.004	1.004	1.010	1.295	1.311	1.217	1.193
6-story-FVD	0.4	1.138	1.043	1.030	1.013	1.301	1.286	1.300	1.273
	0.7	1.097	1.036	1.052	1.040	1.297	1.483	1.328	1.302
	1.0	0.963	1.001	1.016	1.031	1.271	1.298	1.338	1.317
		3-story-FVD		3-story reference		6-story-FVD		6-story reference	
9-story reference	-	1.020	1.013	0.995	1.011	0.925	0.971	0.927	0.995
9-story-FVD	0.4	1.000	1.022	0.998	1.022	0.948	0.996	0.932	1.016
	0.7	0.987	1.012	0.977	0.983	0.931	1.080	0.781	0.815
	1.0	0.958	0.998	0.938	0.942	0.902	0.992	0.867	0.892

Table 6 presents the modification factors of all structures considering pounding with the adjacent structure for the distances equal to 0.0 and 1.0*D*. According to the table, in the case of pounding between 9-, and 6-story-FVD structures for the separation distance of 0.0, the median collapse capacity of 9-story-FVD structure should be reduced by using the modification factor of 0.931. On the contrary, the median collapse capacity of the 6-story-FVD structure can be increased by applying the modification factor of 1.297.

5. Conclusions

The effects of using FVDs have been investigated in the present paper focusing on the seismic performance of two and three adjacent colliding SMRFs considering three different separation distances. The structures were retrofitted with linear and nonlinear FVDs, with values of velocity exponent from 0.4 to 1.0, in order to enhance their seismic performance. Regarding this purpose, the colliding structures were subjected to near-field ground motion records and the modification factors, intended to be used to estimate the influence of pounding on the collapse capacity of structures, were proposed. The results obtained are summarized as follows:

- It is possible to predict the collapse capacity of a structure in pounding condition, when it is retrofitted with linear or nonlinear FVDs, without involving complicated modeling and analytical difficulties. To estimate the effects of pounding on the collapse capacities of adjacent structures, as a function of separation distance, the proposed modification factors can be successfully used.
- The median collapse capacities of structures without any adjacent structure shows an increasing trend for either linear or nonlinear FVDs. Moreover, linear FVDs have a larger influence on the median collapse capacities of structures than the nonlinear FVDs.
- The increase in values of velocity exponent leads to an increase in the median collapse capacity for all colliding structures. Moreover, in the case of pounding between a short structure and a taller one, the increase in the separation distance results in an increase in the median collapse capacity of the taller structure, while the median collapse capacity of the shorter structure decreases correspondingly.
- The seismic collapse probabilities of structures with FVDs are lower than those for structures without FVDs. Moreover, structures with linear FVDs have lower seismic collapse probabilities than structures with nonlinear FVDs.
- Using linear FVDs in taller structure increases the median collapse capacities of both structures. In contrast, using linear FVDs in shorter structure can increase the median collapse capacity of shorter structure alone, but the median collapse capacity of the taller structure remains unchanged.
- Considering two adjacent structures at both sides of the main taller or shorter structure considerably increases the median collapse capacity of the main structure itself. Moreover, in such a case, the decrease in the seismic collapse probability of the main taller or shorter structure can be observed. Also, considering two adjacent structures at one side of the main structure significantly decreases the median collapse capacity of the main structure itself.

This research did not receive any specific grant from funding agencies in the public, commercial, or not-for-profit sectors.

CRediT authorship contribution statement

F. Kazemi: Conceptualization, Methodology, Software, Formal analysis, Investigation, Writing - original draft. **B. Mohebi:** Conceptualization, Methodology, Validation, Formal analysis, Writing - original draft. **R. Jankowski:** Conceptualization, Methodology, Validation, Writing - review & editing.

Declaration of Competing Interest

The authors declare that they have no known competing financial interests or personal relationships that could have appeared to influence the work reported in this paper.

References

[1] R. Jankowski, S. Mahmoud, Earthquake-Induced Structural Pounding, Springer, Cham, Switzerland, 2015.
[2] J.M. Kelly, Base isolation: linear theory and design, Earthq. Spec. 6 (2) (1990) 223–244.
[3] E. Aydin, M.H. Boduroglu, Optimal placement of steel diagonal braces for upgrading the seismic capacity of existing structures and its comparison with optimal dampers, J. Constr. Steel Res. 64 (1) (2008) 72–86.
[4] G.P. Cimellaro, H. Roh, A. De Stefano, Spectral and fragility evaluations of retrofitted structures through strength reduction and enhanced damping, Earthq. Eng. Eng. Vib. 8 (1) (2009) 115–125.
[5] A. Palmeri, G. Muscolino, A numerical method for the time-domain dynamic analysis of buildings equipped with viscoelastic dampers, Struc. Con. Heal. Monitor. 18 (5) (2011) 519–539.
[6] C.A. Martínez, O. Curadelli, M.E. Compagnoni, Optimal design of passive viscous damping systems for buildings under seismic excitation, J. Constr. Steel Res. 90 (2013) 253–264.
[7] O. Lavan, O. Amir, Simultaneous topology and sizing optimization of viscous dampers in seismic retrofitting of 3D irregular frame structures, Earthq. Eng. Struct. Dyn. 43 (9) (2014) 1325–1342.

[8] T. Falborski, R. Jankowski, Experimental study on effectiveness of a prototype seismic isolation system made of polymeric bearings, App. Sci. 7 (8) (2017) 808.
[9] T. Falborski, R. Jankowski, Advanced hysteretic model of a prototype seismic isolation system made of polymeric bearings, App. Sci. 8 (3) (2018) 400.
[10] H. Naderpour, N. Naji, D. Burkacki, R. Jankowski, Seismic response of high-rise buildings equipped with base isolation and non-traditional tuned mass dampers, App. Sci. 9 (6) (2019) 1201.
[11] E. Nastri, M. D'Aniello, M. Zimbru, S. Streppone, R. Landolfo, R. Montuori, V. Piluso, Seismic response of steel Moment Resisting Frames equipped with friction beam-to-column joints, Soil Dyn. Earthq. Eng. 119 (2019) 144–157.
[12] G. De Matteis, G. Brando, F. Caldoso, F. D'Agostino, Seismic performance of dual steel frames with dissipative metal shear panels, Ingegneria Sismica 35 (2) (2018) 124–141.
[13] E. Pavlou, M.C. Constantinou, Response of nonstructural components in structures with damping systems, J. Struc. Eng. 132 (7) (2006) 1108–1117.
[14] O. Lavan, G.F. Dargush, Multi-objective evolutionary seismic design with passive energy dissipation systems, J. Earthq. Eng. 13 (6) (2009) 758–790.
[15] K. Bigdeli, W. Hare, S. Tesfamariam, Configuration optimization of dampers for adjacent buildings under seismic excitations, Eng. Optim. 44 (12) (2012) 1491–1509.
[16] M. Martinez-Rodrigo, M.L. Romero, An optimum retrofit strategy for moment resisting frames with nonlinear viscous dampers for seismic applications, Eng. Struct. 25 (7) (2003) 913–925.
[17] A. Dall'Asta, E. Tubaldi, L. Ragni, Influence of the nonlinear behavior of viscous dampers on the seismic demand hazard of building frames, Earthq. Eng. Struct. Dyn. 45 (1) (2016) 149–169.
[18] E. Tubaldi, M. Barbato, A. Dall'Asta, Performance-based seismic risk assessment for buildings equipped with linear and nonlinear viscous dampers, Eng. Struct. 78 (2014) 90–99.
[19] E. Tubaldi, M. Barbato, S. Ghazizadeh, A probabilistic performance-based risk assessment approach for seismic pounding with efficient application to linear systems, Struc. Safe. 36-37 (2012) 14–22.
[20] M.R. Mansoori, A.S. Moghadam, Using viscous damper distribution to reduce multiple seismic responses of asymmetric structures, J. Constr. Steel Res. 65 (12) (2009) 2176–2185.
[21] Jinkoo Kim, Joonho Lee, Hyungoo Kang, Seismic retrofit of special truss moment frames using viscous dampers, J. Constr. Steel Res. 123 (2016) 53–67.
[22] Luca Landi, Simone Lucchi, Pier Paolo Diotallevi, A procedure for the direct determination of the required supplemental damping for the seismic retrofit with viscous dampers, Eng. Struct. 71 (2014) 137–149.
[23] Luca Landi, Cristina Vorabbi, Omar Fabbri, Pier Paolo Diotallevi, Simplified probabilistic seismic assessment of RC frames with added viscous dampers, Soil Dyn. Earthq. Eng. 97 (2017) 277–288.
[24] Andrea Dall'Asta, Fabrizio Scozzese, Laura Ragni, Enrico Tubaldi, Effect of the damper property variability on the seismic reliability of linear systems equipped with viscous dampers, Bull. Earthq. Eng. 15 (11) (2017) 5025–5053.
[25] Theodore L. Karavasilis, Assessment of capacity design of columns in steel moment resisting frames with viscous dampers, Soil Dyn. Earthq. Eng. 88 (2016) 215–222.
[26] Angelos S. Tzimas, Athanasios I. Dimopoulos, Theodore L. Karavasilis, EC8-based seismic design and assessment of self-centering post-tensioned steel frames with viscous dampers, J. Constr. Steel Res. 105 (2015) 60–73.
[27] Elif Cagda Kandemir-Mazanoglu, Kemal Mazanoglu, An optimization study for viscous dampers between adjacent buildings, Mech. Syst. Sign. Process. 89 (2017) 88–96.
[28] F. Kazemi, M. Miari, R. Jankowski, Investigating the effects of structural pounding on the seismic performance of adjacent RC and steel MRFs, Bull. Earthq. Eng. 19 (1) (2021) 317–343.
[29] Stavros A. Anagnostopoulos, Konstantinos V. Spiliopoulos, An investigation of earthquake induced pounding between adjacent buildings, Earthq. Eng. Struct. Dyn. 21 (4) (1992) 289–302.
[30] K.T. Chau, X.X. Wei, X. Guo, C.Y. Shen, Experimental and theoretical simulations of seismic poundings between two adjacent structures, Earthq. Eng. Struct. Dyn. 32 (4) (2003) 537–554.
[31] Mahmoud Miari, Kok Keong Choong, Robert Jankowski, Seismic pounding between adjacent buildings: Identification of parameters, soil interaction issues and mitigation measures, Soil Dyn. Earthq. Eng. 121 (2019) 135–150.
[32] Vincent Crozet, Ioannis Politopoulos, Mingguan Yang, Jean-Marc Martinez, Silvano Erlicher, Sensitivity analysis of pounding between adjacent structures, Earthq. Eng. Struct. Dyn. 47 (1) (2018) 219–235.
[33] Chris G. Karayannis, Maria J. Favvata, Earthquake-induced interaction between adjacent reinforced concrete structures with non-equal heights, Earthq. Eng. Struct. Dyn. 34 (1) (2005) 1–20.
[34] Maria J. Favvata, Minimum required separation gap for adjacent RC frames with potential inter-story seismic pounding, Eng. Struct. 152 (2017) 643–659.
[35] Christoph Adam, Clemens Jäger, Seismic collapse capacity of basic inelastic structures vulnerable to the P-delta effect, Earthq. Eng. Struct. Dyn. 41 (4) (2012) 775–793.
[36] Christoph Adam, David Kampenhuber, Luis F. Ibarra, Optimal intensity measure based on spectral acceleration for P-delta vulnerable deteriorating frame structures in the collapse limit state, Bull. Earthq. Eng. 15 (10) (2017) 4349–4373.
[37] Farzin Kazemi, Benyamin Mohebi, Mansoor Yakhchalian, Evaluation the P-delta effect on collapse capacity of adjacent structures subjected to far-field ground motions, Civ. Eng. J. 4 (5) (2018) 1066, https://doi.org/10.28991/cej-0309156.
[38] F. Kazemi, B. Mohebi, M. Yakhchalian, Predicting the seismic collapse capacity of adjacent structures prone to pounding, Canad. J. Civil Eng. 47 (6) (2020) 663–677.
[39] B. Mohebi, F. Kazemi, M. Yakhchalian, Investigating the P-Delta effects on the seismic collapse capacity of adjacent structures, in: 16th European Conference on Earthquake Engineering (16ECEE), 18–21, June, Thessaloniki, Greece, 2018.
[40] Armin Masroor, Gilberto Mosqueda, Assessing the collapse probability of base-isolated buildings considering pounding to moat walls using the FEMA P695 methodology, Earthq. Spec. 31 (4) (2015) 2069–2086.
[41] Hytham Elwardany, Ayman Seleemah, Robert Jankowski, Seismic pounding behavior of multi-story buildings in series considering the effect of infill panels, Eng. Struct. 144 (2017) 139–150.
[42] Hytham Elwardany, Ayman Seleemah, Robert Jankowski, Saher El-khoriby, Influence of soil-structure interaction on seismic pounding between steel frame buildings considering the effect of infill panels, Bull. Earthq. Eng. 17 (11) (2019) 6165–6202.
[43] Shoma Kitayama, Michael C. Constantinou, Probabilistic collapse resistance and residual drift assessment of buildings with fluidic self-centering systems, Earthq. Eng. Struct. Dyn. 45 (12) (2016) 1935–1953.
[44] Minimum Design Loads for Buildings and Other Structures (ASCE/SEI 7-10), first, second, and third printings. (2010). Minimum Design Loads for Buildings and Other Structures.
[45] B. Mohebi, O. Yazdanpanah, F. Kazemi, A. Formisano, Seismic damage diagnosis in adjacent steel and RC MRFs considering pounding effects through improved wavelet-based damage-sensitive feature, J. Build. Eng. 101847 (2020).
[46] Neda Asgarkhani, Mansoor Yakhchalian, Benyamin Mohebi, Evaluation of approximate methods for estimating residual drift demands in BRBFs, Eng. Struct. 224 (2020) 110849, https://doi.org/10.1016/j.engstruct.2020.110849.
[47] Masood Yakhchalian, Neda Asgarkhani, Mansoor Yakhchalian, Evaluation of deflection amplification factor for steel buckling restrained braced frames, J. Build. Eng. 30 (2020) 101228, https://doi.org/10.1016/j.jobe.2020.101228.
[48] Dimitrios G. Lignos, Helmut Krawinkler, Deterioration modeling of steel components in support of collapse prediction of steel moment frames under earthquake loading, J. Struc. Eng. 137 (11) (2011) 1291–1302.
[49] James D. Newell, Chia-Ming Uang, Cyclic behavior of steel wide-flange columns subjected to large drift, J. Struct. Eng. 134 (8) (2008) 1334–1342.

[50] Choung-Yeol Seo, Theodore L. Karavasilis, James M. Ricles, Richard Sause, Seismic performance and probabilistic collapse resistance assessment of steel moment resisting frames with fluid viscous dampers, Earthq. Eng. Struct. Dyn. 43 (14) (2014) 2135–2154.
[51] Shoma Kitayama, Michael C. Constantinou, Design and analysis of buildings with fluidic self-centering systems, J. Struct. Eng. 142 (11) (2016) 04016105, https://doi.org/10.1061/(ASCE)ST.1943-541X.0001583.
[52] Luca Landi, Filippo Conti, Pier Paolo Diotallevi, Effectiveness of different distributions of viscous damping coefficients for the seismic retrofit of regular and irregular RC frames, Eng. Struct. 100 (2015) 79–93.
[53] A. Yahyazadeh, M. Yakhchalian, Probabilistic residual drift assessment of SMRFs with linear and nonlinear viscous dampers, J. Constr. Steel Res. 148 (2018) 409–421.
[54] H.R. Jamshidiha, M. Yakhchalian, B. Mohebi, Advanced scalar intensity measures for collapse capacity prediction of steel moment resisting frames with fluid viscous dampers, Soil Dyn. Earthq. Eng. 109 (2018) 102–118.
[55] Sayed Mahmoud, Xiaojun Chen, Robert Jankowski, Structural pounding models with Hertz spring and nonlinear damper, Journal of App. Sci. 8 (10) (2008) 1850–1858.
[56] B. Sołtysik, R. Jankowski, Non-linear strain rate analysis of earthquake-induced pounding between steel buildings, Inter. J. Earth Sci. Eng. 6 (3) (2013) 429–433.
[57] Hossein Rezaei, Seyyed Amirhossein Moayyedi, Robert Jankowski, Probabilistic seismic assessment of RC box-girder highway bridges with unequal-height piers subjected to earthquake-induced pounding, Bull. Earthq. Eng. 18 (4) (2020) 1547–1578.
[58] Panayiotis C. Polycarpou, Petros Komodromos, Earthquake-induced poundings of a seismically isolated building with adjacent structures, Eng. Struct. 32 (7) (2010) 1937–1951.
[59] F. McKenna, G.L. Fenves, F.C. Filippou, M.H. Scott, Open system for earthquake engineering simulation (OpenSees), Berkeley, Pacific Earthquake Engineering Research Center, University of California, 2016. Web page. http://OpenSees.berkeley.edu.
[60] Stavros A. Anagnostopoulos, Pounding of buildings in series during earthquakes, Earthq. Eng. Struct. Dyn. 16 (3) (1988) 443–456.
[61] Stavros A. Anagnostopoulos, Equivalent viscous damping for modeling inelastic impacts in earthquake pounding problems, Earthq. Eng. Struct. Dyn. 33 (8) (2004) 897–902.
[62] S.A. Anagnostopoulos, C.E. Karamaneas, Use of collision shear walls to minimize seismic separation and to protect adjacent buildings from collapse due to earthquake-induced pounding, Earthq. Eng. Struct. Dyn. 37 (12) (2008) 1371–1388.
[63] Panayiotis C. Polycarpou, Loizos Papaloizou, Petros Komodromos, An efficient methodology for simulating earthquake-induced 3D pounding of buildings, Earthq. Eng. Struct. Dyn. 43 (7) (2014) 985–1003.
[64] M.M. Salman, A.H. Al-Amawee, The ratio between static and dynamic modulus of elasticity in normal and high strength concrete, J. Eng. Sust. Develop. 10 (2) (2006) 163–174.
[65] F. Kazemi, B. Mohebi, M. Yakhchalian, Enhancing the seismic performance of adjacent pounding structures using viscous dampers, in: 16th European Conference on Earthquake Engineering (16ECEE), 18–21, June, Thessaloniki, Greece, 2018.
[66] MATLAB/Simulink as a Technical Computing Language. Engineering Computations and Modeling in MATLAB, 2016.
[67] Dimitrios Vamvatsikos, C. Allin Cornell, Incremental dynamic analysis, Earthq. Eng. Struct. Dyn. 31 (3) (2002) 491–514.
[68] Alban Kita, Nicola Cavalagli, Maria Giovanna Masciotta, Paulo B. Lourenço, Filippo Ubertini, Rapid post-earthquake damage localization and quantification in masonry structures through multidimensional non-linear seismic IDA, Eng. Struct. 219 (2020) 110841, https://doi.org/10.1016/j.engstruct.2020.110841.
[69] M. Yakhchalian, A. Nicknam, G.G. Amiri, Proposing an optimal integral-based intensity measure for seismic collapse capacity assessment of structures under pulse-like near-fault ground motions, J. Vibro. 16 (3) (2014) 1245.